12th IFAC International Symposium on
Advanced Control of Chemical Processes
July 14-17, 2024. Toronto, Canada

A simplified dynamic model of direct stem generation solar plants for state estimation and control applications ⋆

Gustavo A. de Andrade * **Paulo H. F. Biazetto** *
Julio E. Normey-Rico *

* *Department of Automation and Systems, Federal University of Santa Catarina, Florianópolis CEP 88040-900, Brazil (e-mail: gustavo.artur@ufsc.br; paulo.biazetto@posgrad.ufsc.br; julio.normey@ufsc.br)*

Abstract: In this work, we propose a simplified model for direct steam generation parabolic trough collector solar plants consisting of a system coupled partial differential equations (PDEs) and ordinary differential equations (ODEs). Particularly, the PDEs represent the behavior of the two-phase gas-liquid flow in the collector field, which was obtained assuming a quasi-equilibrium on the mixture momentum balance of the classical transient homogeneous equilibrium model. The gas-liquid separator is given by ODEs obtained from the mass and energy balance laws. This formulation makes the model attractive for optimization and control applications since it is simpler than other approaches in the literature. Finally, in view of the obtained simulation results, the main uses and applications of the developed model are drawn describing a simulation example that proves how the closed-loop operation allows for obtaining higher production rates.

Keywords: Solar energy, Parabolic Trough Collector, Direct Steam Generation, Modeling, Model Reduction

1. INTRODUCTION

Direct steam generation (DSG) process is a concentrated solar power (CSP) plant type that is considered one of the most promising technologies of the next-generation CSP plants. Unlike the heat transfer fluid (HTF) technologies, where the HTF (normally synthetic oil or molten salt) serves as intermediate for heat transfer, in DSG plants, water is directly heated by concentrated solar radiation to generate steam. This leads to the following advantages over classic CSP plants (Fernández-García et al., 2010): (i) no environmental risk of fire and leakage; (ii) a maximum temperature for the thermodynamic cycle can be achieved of over 400 °C; (iii) the overall plant efficiency can be higher, since there is no oil/steam heat exchanger; and (iv) operation and maintenance costs are lower than for a synthetic oil based plant.

As shown in Sun et al. (2015), the above advantages could help to reduce the costs of the power produced in CSP plants by about 15%. However, the two-phase flow behavior in DSG plants makes its operation and feedback control design challenging. In particular, strong transients in solar radiation make it difficult to regulate the steam temperature because of the constraints on the minimum feed flow rate and high temperature gradients inside the absorber tubes. Additionally, the water flow injection must be well controlled to avoid stratified flow in the evaporation stage. Thus, to improve system performance with a robust operation strategies, it is necessary to design advanced control methodologies that take into account the mixing and mass transfer phenomena that occur in the system. For this reason, suitable models are required to design controllers that improve the operational conditions of the plant (Biazetto et al., 2023).

In general, one-dimensional partial differential equations (PDEs) approaches are the only affordable concept to address full-scale plant simulations under a wide range of circumstances in transient conditions de Andrade et al. (2015). The formulations for two-phase flow regimes are traditionally given by the homogeneous equilibrium model (HEM), drift-flux, or two-fluid models, however, the HEM is the most used approach for the study of DSG plants due to its low complexity (De Sá et al., 2018). Experimental validations of the HEM approach using in-house codes in different DSG test facilities, for both summer and winter days, can be seen in Yan et al. (2010); Guo et al. (2017), and the references therein. Mathematical models developed with commercial software, such as RELAP5 and Modelica, were also explored in the context of DSG systems, as presented in Eck and Hirsch (2007); Serrano-Aguilera et al. (2017). Although these articles show good quantitative results, the models become very complex for controller design because of their nonlinearities, boundary conditions and couplings.

This work proposes a simplified first principle dynamic model based on PDEs and ordinary differential equations

⋆ The authors thanks the brazilian agencies CNPq and CAPES that have partially funded the research under projects: CNPq 158803/2021-3, CNPq 403949/2021-1, CNPq 406477/2022-1, CNPq 304032/2019-0, CAPES/Print/Automação 4.0, and CAPES 88881.878833/2023-01.

for DSG systems operating in recirculation mode. The model takes into account the thermohydraulic characteristics of the system and predicts the most important variables, such as temperature, pressure, steam quality, and velocity, that influence the performance of any DSG plant. The multiphase flow along the preheating and superheating stages is described by a simplified version of the HEM formulation, where the static momentum balance for the mixture is imposed. As we shall see, this allows us to reduce the multiphase flow dynamic equations into a set of two PDEs that describe thermal energy inside the tubes along with static relationships of steam velocity and pressure. The dynamics of the plant's water/vapor separator is modeled by two ODEs which describe the water/steam volume and pressure inside the separator. The coupling between the equations is given through suitable boundary conditions and the resulting PDE-ODE system can be implemented with robust, simple, and fast numerical approaches. The proposed model is validated with the experimental data described in Zarza et al. (2006). Additionally, numerical simulations for the plant operating in closed-loop over a day are presented.

The rest of the paper is organized as follows. In Section 2 we describe the DSG solar plant and its control problem. The mathematical model and its reduction are presented in Section 3. Simulation results of the proposed model under real data disturbances are shown in Section 4. Finally, the concluding remarks and directions of future works are given in Section 5.

2. SYSTEM DESCRIPTION

The recirculation DSG parabolic trough collector solar plant considered in this work is depicted in Figure 1. Basically, the system consists of a solar field, a water/steam separator and an attemperator. The solar collector field is assembled by several parabolic trough collectors. A water-steam separator is installed at the end of the evaporator section of the collector loop so that the water is recirculated to the collector loop inlet. The excess water in the evaporator section guarantees good wetting of the absorber tubes and makes stratification impossible. The steam produced is separated from the water by the separator and fed into the inlet of the superheating section. The spray attemperator is installed at the inlet of the last collector assembly to control the temperature of the outlet steam. The section of collector row between the separator and the spray attemperator is defined as the primary superheater and the section after the spray attemperator is named as the secondary superheater.

For the proper and safe operation of the system, variables must be regulated around their operating points. In DSP plants, the main control objective is to maintain the outlet steam at a constant temperature of the solar field despite solar radiation variations and inlet water conditions. The main control loops are Valenzuela et al. (2005):

- Water/steam separator liquid level control loop: the feed flow is adjusted to maintain the level around a nominal value avoiding high or low levels inside the tank. Variations in solar radiation highly affect this loop, since the steam production and the tank level vary when the radiation changes.
- Outlet steam temperature control loop: The outlet steam temperature of the superheater is adjusted by water injection in the inlet of the last collector (see Figure 1).

3. MATHEMATICAL MODELING

In this section, we propose a mathematical model of the recirculation DSG plant. Each of the subsystems of the plant, namely, the preheater, the first and secondary superheaters, the spray attemperator, and the water/steam separator will be modeled by a set of differential equations coupled by suitable boundary conditions. The subindex $i \in \{ph, ws, ps, ss\}$ will be used to represent the variables corresponding to the preheater, water/steam separator, primary superheater, and secondary superheater, respectively.

3.1 Energy balance of the absorber tube

The solar plant concentrates direct solar irradiation onto the wall of absorber tube through the glass envelope and the evaluated space. Thus, applying the energy balance in the tube walls, we obtain the following equation for its temperature dynamics:

$$\rho_{at,i} C_{at,i} A_{at} \frac{\partial T_{at,i}}{\partial t}(t,z) = Q_{sol}(t) - Q_{amb,i}(t,z) - Q_{f,i}(t,z), \quad (1)$$

where $t \in [0, \infty)$ is the time and $z \in [L_{j-1}, L_j]$ is the space, with $j \in \{1,2,3,4\}$. The density, specific heat and temperature of the absorber tube are given by $\rho_{at,i}$, $C_{at,i}$ and $T_{at,i}$, respectively. The cross-sectional area is A_{at} and the terms $Q_{sol,i}$, $Q_{f,i}$ and $Q_{amb,i}$ represent the solar radiation absorbed, the heat transfer with the water flowing into the absorber and the heat transfer to the atmosphere, respectively. In this work, the thermal losses of the EuroTrough collector using a UVAC absorber are considered (Lupfert et al., 2003):

$$Q_{sol}(t) = \eta G I(t), \quad (2)$$

$$Q_{f,i}(t,z) = \pi d_i c_i (T_{at,i}(t,z) - T_i(t,z)), \quad (3)$$

$$Q_{amb,i}(t,z) = A + B(T_{at,i}(t,z) - T_{amb}(t)) + C(T_{at,i}(t,z) - T_{amb}(t))^2, \quad (4)$$

where I is the solar irradiation T_{amb} is the ambient temperature and T_i is the fluid temperature. The collector efficiency and the collector aperture are given by η and G, respectively. The inner tube diameter is d_i, whereas c_i is heat transfer coefficient, and A, B and C are fitting parameters. Importantly, the solar radiation and ambient temperature are assumed to be measured variables.

The expressions for the computation of c_i in (3) will be given in the next section after the dynamic model of the multiphase flow inside the absorber tube is presented.

Finally, the initial condition of (1) is given by

$$T_{at,i}(0,z) = T_{at,i,0}(z), \quad (5)$$

where $T_{at,i,0} \in \mathcal{C}^1(L_{j-1}, L_j)$, for $j \in \{1, \ldots, 4\}$ is a given function.

3.2 Four-equation model for the water flow

In this work, the water flow inside the absorber tube is modeled with the classical four-equation formulation:

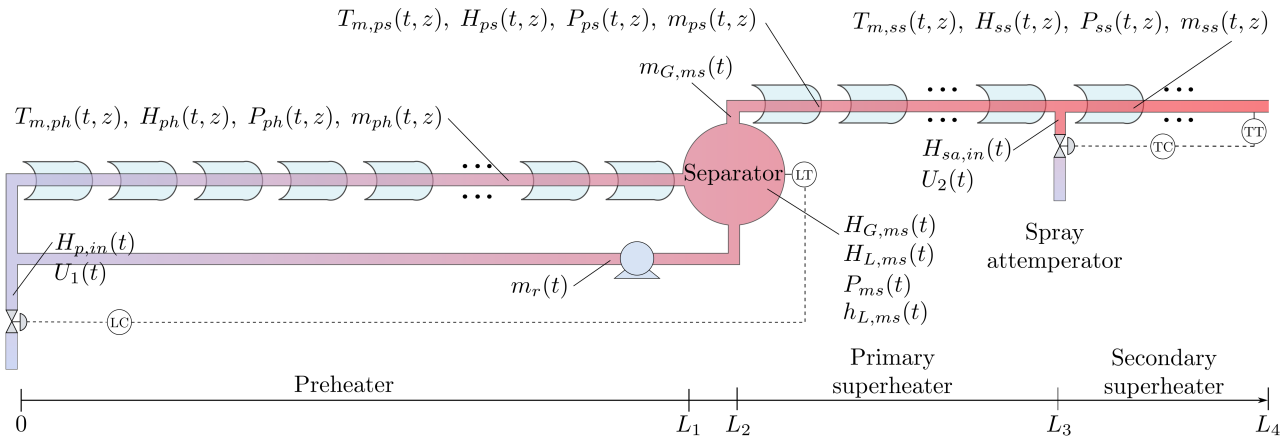

Fig. 1. A schematic diagram of the PTC plant.

$$\frac{\partial \alpha_{G,i}\rho_{G,i}}{\partial t}(t,\,z) + \frac{\partial \alpha_{G,i}\rho_{G,i}v_i}{\partial z}(t,\,z) = 0, \tag{6}$$

$$\frac{\partial \alpha_{L}\rho_{L,i}}{\partial t}(t,\,z) + \frac{\partial \alpha_{L,i}\rho_{L,i}v_i}{\partial z}(t,\,z) = 0, \tag{7}$$

$$\frac{\partial P_i}{\partial z}(t,z) = S_i(t,z), \tag{8}$$

$$A_i\rho_i(t,\,z)\frac{\partial H_i}{\partial t}(t,\,z) + m_i(t,z)\frac{\partial H_i}{\partial z}(t,\,z) = Q_{f,i}(t,z), \tag{9}$$

where $\alpha_{j,i}$, $\rho_{j,i}$ are the volume fraction and density of phase $j \in \{G, L\}$ (gas or liquid), respectively, whereas ρ_i, v_i, m_i, P_i, and H_i are the density, velocity, mass flow rate, pressure and enthalpy of the mixture. The momentum source term, S_i, is given by

$$S_i(t,\,z) = -A_i\rho_i(t,\,z)g\sin\left(\theta(z)\right) - \frac{f_i(t,z)m_i(t,z)^2}{2A_i\rho_i(t,z)d_i}, \tag{10}$$

in which g is the acceleration of gravity and f_i is the friction term, which can be computed using the Colebrook equation.

In the formulation (6)-(9), the two-phase flow is assumed as a homogeneous mixture in thermal equilibrium, where no relative velocity is considered between both phases. As a consequence, the following relations are valid:

$$\alpha_{L,i}(t,\,z) + \alpha_{G,i}(t,\,z) = 1, \tag{11}$$

$$x_i(t,\,z) = \frac{H_i(t,\,z) - H_{L,i}(t,\,z)}{H_{G,i}(t,\,z) - H_{L,i}(t,\,z)}, \tag{12}$$

$$\rho_i(t,\,z) = \alpha_{G,i}(t,\,z)\rho_{G,i}(t,\,z) + \alpha_{L,i}(t,\,z)\rho_{L,i}(t,\,z), \tag{13}$$

$$H_i(t,\,z) = x_i(t,\,z)H_{G,i}(t,\,z) + (1 - x_i(t,\,z))H_{L,i}(t,\,z). \tag{14}$$

The thermodynamic properties of (6)-(14) can be obtained from the corresponding thermodynamic state equations for water, e.g., IAPWS-IF97 formulation, which depends on pressure and enthalpy.

In order to obtain a well-posed problem for the PDE system (6)-(9), initial and boundary conditions must be imposed. For the initial condition, we consider that

$$\begin{aligned} \alpha_{G,i}(0,z) &= \alpha_{0,i}(z), \qquad & P_i(0,z) &= P_{0,i}(z), \\ v_i(0,z) &= v_{0,i}(z), \qquad & H_i(0,z) &= H_{0,i}(z), \end{aligned} \tag{15}$$

where $\alpha_{0,i}$, $P_{0,i}$, $v_{0,i}$, $H_{0,i} \in \mathcal{C}^1((L_{j-1}, L_j))$, for $j \in \{1,\ldots,4\}$, are given.

The boundary conditions of the solar plant are more delicate, as the coupling between subsystems and exogenous variables must be taken into account so that the dynamic behavior of the model is correct. Next, we will present the boundary conditions used in this work.

Preheating section: in this case, the boundary conditions are

$$\begin{aligned} m_{ph}(t,0) &= U_1(t) + m_r(t), \qquad & P_{ph}(t,L_1) &= P_{ws}(t), \\ H_{ph}(t,0) &= \frac{U(t)H_{L,in}(t) + m_r(t)H_{L,ms}(t)}{U_1(t) + m_r(t)}, \end{aligned} \tag{16}$$

where U_1 is the prescribed mass flow rate at the inlet of the solar field (control variable), m_r is the recirculation mass flow rate, $H_{L,in}$ is the inlet enthalpy, and P_{ws} is the water/steam separator pressure.

Primary superheater section: this subsystem is connected with the water/steam separator and the secondary superheater. Thus, its boundary conditions are

$$\begin{aligned} m_{ps}(t,L_2) &= m_{G,ms}(t), \qquad & H_{ps}(t,L_2) &= H_{G,ms}(t), \\ P_{ps}(t,L_3) &= P_{ss}(t,L_3), \end{aligned} \tag{17}$$

where $m_{G,ms}$ is the separator outlet steam mass flow rate, $H_{G,ms}$ is the steam enthalpy in the separator and P_{ss} is the pressure at the secondary superheater.

Secondary superheater section: this part of the system is coupled with the spray attemperator, the primary superheater, and the final separator. Therefore, the boundary conditions are given by

$$\begin{aligned} m_{ss}(t,L_3) &= m_{ps}(t,L_3) + U_2(t), \qquad & P_{ss}(t,L_4) &= P_{fs}(t), \\ H_{ss}(t,L_3) &= \frac{m_{ps}(t,L_3)H_{ps}(t,L_3) + U_2(t)H_{L,sa}(t)}{m_{ps}(t,L_3) + U_2(t)}, \end{aligned} \tag{18}$$

where U_2 is the prescribed mass flow rate at spray attemperator (control variable), $H_{L,sa}$ is the enthalpy of water at the spray attemperator, and P_{fs} is the pressure at the final separator.

Explicit Pressure Profile

Integrating (8) along the space $z \in [L_{i-1}, L_i]$, for $i \in \{1,\ldots,4\}$, and plugging the corresponding boundary condition we get

$$P_i(t,\,z) = P_{L_i}(t) + \int_{L_i}^{z} S_i(t,\xi)d\xi. \tag{19}$$

where P_{L_i} stands for the pressure boundary condition of the i-th subsystem (see (16), (17) and (18)).

Note that this expression is implicit, since S_i is dependent on v_i which is in turn dependent on $\rho_{G,i}$. To avoid this complication a simplification should be used, e.g. by assuming $m_i(t,z)$ uniform in space and equal to its boundary condition when calculating the pressure profile, that is, $m_i(t,z) = m_{L_i}(t)$, where m_{L_i} is mass flow rate boundary condition of the i-th subsystem (see (16), (17) and (18)). Then,

$$S_i(z) \approx -\bar{\rho}_i(z)\left(g\sin(\theta(z)) + \frac{f_i m_{L_i}^2}{2d_i}\right), \tag{20}$$

with $\bar{\rho}_i(z) = \bar{\rho}_{L,i}\alpha_{L,i}(z) + \bar{\rho}_{G,i}\alpha_{G,i}(z)$, i.e. a mean approximate liquid and gas density is used. This makes the source term S_i explicit in $\alpha_{G,i}$ and in the boundary condition m_{L_i}.

Explicit Velocity Profile

We get from (7), assuming that $\rho_{L,i}$ is constant and using the relation $\alpha_{L,i} + \alpha_{G,i} = 1$,

$$\frac{\partial \alpha_{G,i}}{\partial t} + v_i\frac{\partial \alpha_{G,i}}{\partial z} = \alpha_{L,i}\frac{\partial v_i}{\partial z}. \tag{21}$$

Note that an explicit expression for $\alpha_{L,i}\frac{\partial v_i}{\partial z}$ can be obtained by applying the chain rule into (6), which in turn, allows as to rewrite (21) as

$$\frac{\partial \alpha_{G,i}}{\partial t} + v_i\frac{\partial \alpha_{G,i}}{\partial z} = -\frac{\alpha_{G,i}\alpha_{L,i}}{\rho_{G,i}}\left(\frac{\partial \rho_{G,i}}{\partial t} + v_i\frac{\partial \rho_{G,i}}{\partial z}\right). \tag{22}$$

Define

$$E_{G,i} = -\frac{\alpha_{G,i}\alpha_{L,i}}{\rho_{G,i}}\left(\frac{\partial \rho_{G,i}}{\partial t} + v_i\frac{\partial \rho_{G,i}}{\partial z}\right). \tag{23}$$

Then, (21) can be simplified to

$$\frac{\partial v_i}{\partial z} = \frac{E_{G,i}}{\alpha_{L,i}}. \tag{24}$$

Next, we use the isentropic bulk modulus property, allowing us to relate gas phase density to pressure, and then (23) can be rewritten to

$$E_{G,i} = -\frac{\alpha_{G,i}\alpha_{L,i}}{\gamma P_i}\left(\frac{\partial P_i}{\partial t} + v_i\frac{\partial P_i}{\partial z}\right). \tag{25}$$

For deriving the velocity, we neglect the $\frac{\partial P_i}{\partial t}$ term from (25). Then, inserting (25) without the transient pressure term into (24), recalling 8,

$$\frac{\partial v_i}{\partial z} = -\frac{\alpha_{G,i}}{\gamma P_i}v_i S_i,$$

and consequently, by defining the integral

$$I_{v,i}(z) = \int_{L_{i-1}}^{z}\frac{\alpha(\theta)}{\gamma P_i(\theta)}S_i(\theta)d\theta,$$

the distributed velocity is obtained as

$$v_i(t,z) = \mathrm{e}^{-I_v(z)}v_i(t,L_{i-1}). \tag{26}$$

3.3 Mathematical model of the water/steam separator

The behavior of this subsystem is captured by mass and energy balances. The separator is of the horizontal cylindrical type with flat sides. A key property of our modeling approach is that all parts of the water/steam separator which are in contact with the saturated liquid-vapor mixture will be in thermal equilibrium. Thus, the energy stored in steam and water is released or absorbed very rapidly when the pressure changes. The rapid release of energy ensures that different parts of the separator change their temperature in the same way. For this reason, the dynamics can be captured by models of low order. In this work, this is done using a lumped parameter model by means of an ODE system.

Applying the mass conservation into the separator we have

$$\frac{d}{dt}(V_{L,ms}(t)\rho_{L,ms}(t) + V_{G,ms}(t)\rho_{G,ms}(t)) = m_{ph}(t,L_1) - m_r(t) - m_{G,ms}(t), \tag{27}$$

whereas the energy conservation equation reads

$$\frac{dE_{ws}}{dt}(t) = m_{ph}(t,L_1)H_{ph}(t,L_1) - m_{G,ms}H_{G,ms}(t) - m_r(t)H_{L,ms}(t), \tag{28}$$

with

$$\begin{aligned}E_{ws}(t) &= V_{L,ws}(t)\rho_{L,ws}(t)H_{L,ws}(t) + \\ &\quad V_{G,ws}(t)\rho_{G,ws}(t)H_{G,ws}(t) + M_{ws}C_{p,ws}T_{ws}(t),\\ V_{ws}(t) &= V_{L,ws}(t) + V_{G,ws}(t).\end{aligned}$$

With (27)-(28) and considering saturated liquid-vapor mixture in thermal equilibrium, we get that the water/steam separator pressure equation can be derived as

$$\frac{dP_{ws}}{dt}(t) = \Big(E_{in}(t) - E_r(t) - E_{out}(t) - N_1(t)(m_{ph}(t,L_1) - m_r(t) - m_{G,ms}(t))\Big)\times \frac{1}{V_{G,ms}(t)D_1(t) + V_{L,ms}(t)D_2(t) + D_3(t)}, \tag{29}$$

where

$$\begin{aligned}E_{in}(t) &= m_{ph}(t,L_1)H_{ph}(t,L_1),\ E_r(t) = m_r(t)H_{L,ws}(t),\\ E_{out}(t) &= m_{G,ws}(t)H_{G,ws}(t),\ r(t) = H_{G,ws}(t) - H_{L,ws}(t),\\ N_1(t) &= \frac{\rho_{G,ws}(t)H_{G,ws}(t) - \rho_{L,ws}(t)H_{L,ws}(t)}{\rho_{G,ws}(t) - \rho_{L,ws}(t)},\\ D_1(t) &= \rho_{G,ws}(t)\frac{\partial H_{G,ws}}{\partial P_{ws}}(t) + \frac{r(t)\rho_{L,ws}(t)}{\rho_{G,ws}(t) - \rho_{L,ws}(t)}\frac{\partial \rho_{G,ws}}{\partial P_{ws}}(t),\\ D_2(t) &= \rho_{L,ws}(t)\frac{\partial H_{L,ws}}{\partial P_{ws}}(t) + \frac{r(t)\rho_{G,ws}(t)}{\rho_{G,ws}(t) - \rho_{L,ws}(t)}\frac{\partial \rho_{L,ws}}{\partial P_{ws}}(t),\\ D_3(t) &= M_{ws}C_{p,ws}\frac{\partial T_{ws}}{\partial P_{ws}}(t).\end{aligned}$$

Finally, the water level of the separator can be obtained by applying a mass balance for the water volume control in the separator:

$$\frac{d}{dt}(\rho_{L,ms}(t)V_{L,ms}(t)) = m_{ph}(t,L_1)(1 - x_{ph}(t,L_1)) - m_r(t). \tag{30}$$

Note that the water volume inside the tank depends on the water level, i.e.,

$$V_{L,ws} = L_{ws}\left(r_{ws}^2\cos^{-1}\left(\frac{r_{ws}-h_{L,ws}}{r_{ws}}\right) - (r_{ws}-h_{L,ws})\sqrt{2r_{ws}h_{L,ms}-h_{L,ws}^2}\right)$$

where $h_{L,ws}$ is the water level inside the separator. Then, (30) can be rewritten to

$$\frac{dh_{L,ws}}{dt}(t) = \frac{m_{ph}(t,L_1)(1-x_{ws}(t,L_1)) - m_r(t)}{\rho_{L,ws}(t)\frac{dV_{L,ws}}{dh_{L,ws}}(t)}, \quad (31)$$

with

$$\frac{dV_{L,ws}}{dh_{L,ws}} = L_{ws}\left[\sqrt{h_{L,ws}(2r_{ws}-h_{L,ws})} + \frac{r_{ws}^2}{\sqrt{h_{L,ws}(2r_{ws}-h_{L,ws})}} - \frac{(r_{ws}-h_{L,ws})^2}{\sqrt{h_{L,ws}(2r_{ws}-h_{L,ws})}}\right].$$

Equations (29) and (31) fully describe the dynamics of the water/steam separator together with the initial conditions

$$P_{ws}(0) = P_{ws,0}, \qquad h_{L,ws}(0) = h_{L,ws,0}, \qquad (32)$$

where $P_{ws,0}$ and $h_{L,ws,0}$ are given constants.

4. SIMULATION RESULTS

In this section, the simulation results of the proposed model are presented for two different scenarios. The first one is to highlight its accuracy with other results in literature, while the second numerical scenario illustrates the feasibility of the model to a typical day of a DSG solar plant operating in a closed-loop framework.

4.1 Static validation

In this numerical scenario, a single loop of INDITEP project Zarza et al. (2006) is simulated. The loop is comprised of 10 collectors and operates in recirculation mode. The steam/water separator is set between the 8th and 9th collectors for recirculation while an injector is set between the 9th and 10th collectors to prevent overheating. The reader interested on other technical data and environmental and working conditions is referred to Zarza et al. (2006). The model calibration was performed by comparison of the real data with the static simulation responses obtained using estimated parameter, such as collector efficiency, heat transfer coefficients and friction losses. A good agreement between the present simulation results and data from Zarza et al. (2006) can be seen in Figure 2.

4.2 Dynamic simulation

The solar radiation and ambient temperature data were borrowed from the SONDA project (INPE, 2018) and correspond to the location of Cachoeira Paulista, in São Paulo, Brazil, with latitude $22°\ 41'\ 22,65''\ S$ and longitude $45°\ 00'\ 22,28''\ O$, and 574 m altitude. The rest of the parameters of the plant were the same as the ones presented in Section 4.1. Two PI controllers with bumpless and anti-windup techniques have been also designed and implemented for the plant for the liquid level control in the separator, and the regulation of the outlet temperature, respectively. For the gains of the controllers, simplified transfer functions have been investigated for the operating point and the PI controller parameters have been designed.

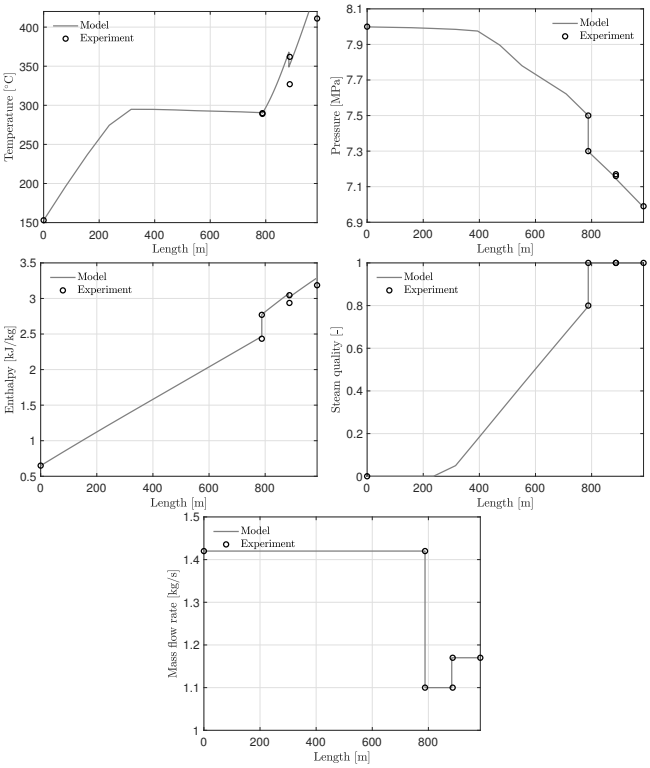

Fig. 2. Validation of the proposed model by data of the INDITEP project Zarza et al. (2006).

In Figure 3 it is depicted the water outlet temperature in the preheater (top graphic), the pressure drop and outlet void fraction in the preheater (middle graphic), and drum water level and preheater inlet flow rate (bottom graphic). During the first hour of this numerical scenario, the water in the preheater was kept recirculating in the solar field until its saturation temperature was reached and steam started to be generated in the plant. Note that the outlet temperature (top graphic of Figure 3) increases from $t = 11$ h to $t = 11.7$ h, then basically stays constant along the rest of the day. Once the plant has started to generate steam, the PI water level controller kicks in and water begins to be injected into the preheater (see the bottom graphic of Figure 3). The control system was able to track the water level reference throughout the entire day (bottom graphic of Figure 3) in spite of the solar radiation and ambient temperature disturbances. The maximum reference error value is around 0.012 m, which can be seen in the third graph of Figure 3 between the time instants $t = 12$ h and $t = 13$ h.

The variables associated with the superheater are shown in Figure 4. As can be seen in the top graphic of Figure 4, the PI controller was able to maintain the outlet steam temperature around the desired reference. During the strong transients of solar radiation (between $t = 12$ h and $t = 14.5$ h) the maximum error value of around 7 °C and the control signal (bottom graphic of Figure 4) was smooth along the entire day. Finally, the pressure drop in

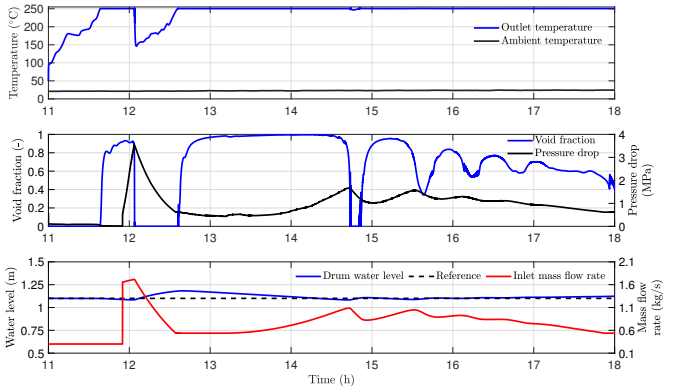

Fig. 3. Simulation results of the proposed model. From top to bottom the graphics show: preheater outlet temperature, ambient temperature, steam quality, solar irradiation, separator water level and inlet mass flow rate.

the superheater can be observed in the middle graphic of Figure 4.

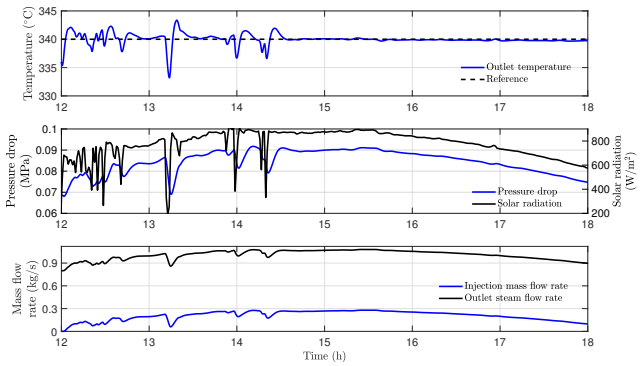

Fig. 4. Simulation results of the proposed model. From top to bottom the graphics show: preheater outlet temperature, ambient temperature, steam quality, solar irradiation, separator water level and inlet mass flow rate.

The model can be used to determine variables that cannot be measured such as the void fraction, vapor quality and heat losses in different sections of the plant. Data obtained from simulations show that the average void fraction inside the preheater is 0.6, whereas the vapor quality is 0.26. The average energy efficiency of this part of the plant is 63.2 % and the steam production has an average value of 0.18 kg/s. Regarding the superheater, the average energy efficiency was 55.4 % for this particular numerical scenario.

5. CONCLUSIONS

In this paper, we introduce a new simplified model for characterizing a collector field operating in recirculation mode with DSG technology. The model builds upon the homogeneous equilibrium model, incorporating simplifications such as a no-pressure-wave model and a quasi-steady pressure and velocity profile. To ensure that the new model preserves essential characteristics related to the original model, a static validation was conducted using real data. Future works may delve into the application of the proposed model from a control strategies perspective, particularly in non-linear predictive control. Another direction to pursue is to extend the model to other DSG topologies.

REFERENCES

Biazetto, P.H.F., de Andrade, G.A., and Normey-Rico, J.E. (2023). Development of an optimal control strategy for temperature regulation and thermal storage operation of a solar power plant based on fresnel collectors. *IEEE Transactions on Control Systems Technology*, 31, 1149–1164.

de Andrade, G.A., Álvarez, J.D., Pagano, D.J., and Berenguel, M. (2015). Nonlinear controllers for solar thermal plants: A comparative study. *Control Engineering Practice*, 43, 12–20.

De Sá, A.B., Pigozzo Filho, V.C., Tadrist, L., and Passos, J.C. (2018). Direct steam generation in linear solar concentration: experimental and modeling investigation–a review. *Renewable and Sustainable Energy Reviews*, 90, 910–936.

Eck, M. and Hirsch, T. (2007). Dynamics and control of parabolic trough collector loops with direct steam generation. *Solar Energy*, 81(2), 268–279.

Fernández-García, A., Zara, E., Valenzuela, L., and Pérez, M. (2010). Parabolic-trough solar collectors and their applications. *Renewable and Sustainable Energy Reviews*, 14, 1695–1721.

Guo, S., Chu, Y., Liu, D., Chen, X., Xu, C., Coimbra, C.F.M., Zhou, L., and Liu, Q. (2017). The dynamic behavior of once-through direct steam generation parabolic trough solar collector row under moving shadow conditions. *Journal of Solar Energy Engineering*, 139(4).

INPE (2018). *Sistema de Organização Nacional de Dados Ambientais*. URL `http://sonda.ccst.inpe.br/basedados/cachoeira.html`. [Accessed 03/22/2021].

Lupfert, E., Zarza, E., Geyer, M., Nava, P., Langenkamp, J., Schiel, W., Esteban, A., Osumar, R., and Mendelberg, E. (2003). Eurotrough collector qualification complete - Performance test results from PSA. In *Proceedings of the ISES 2003 Solar World Congress*, 4903–4908.

Serrano-Aguilera, J.J., Valenzuela, L., and Parras, L. (2017). Thermal hydraulic RELAP5 model for a solar direct steam generation system based on parabolic trough collectors operating in once-through mode. *Energy*, 133, 796–807.

Sun, J., Liu, Q., and Hong, H. (2015). Numerical study of parabolic-trough direct steam generation loop in recirculation mode: Characteristics, performance and general operation strategy. *Energy Conversion and Management*, 96, 287–302.

Valenzuela, L., Zarza, E., Berenguel, M., and Camacho, E.F. (2005). Control concepts for direct steam generation in parabolic troughs. *Solar Energy*, 78(2), 301–311.

Yan, Q., Hu, E., Yang, Y., and Zhai, R. (2010). Dynamic modeling and simulation of a solar direct steam-generating system. *International journal of energy research*, 34(15), 1341–1355.

Zarza, E., Rojas, M.E., Gonzalez, I., Caballero, J.M., and Rueda, F. (2006). INDITEP: The firstpre-commercial DSG solar power plant. *Solar Energy*, 80, 1270–1276.